Comparison of rovibronic density of asymmetric versus symmetric NO_2 isotopologues at dissociation threshold: Broken symmetry effects

R. Jost
Laboratoire de Spectrométrie Physique, Centre National de la Recherche Scientifique-Unité Mixte de Recherche (CNRS-UMR) 5588, Université Joseph Fourier-Grenoble 1, BP 87, 38402 Saint Martin d'Hères Cedex, France

G. Michalski[a] and M. Thiemens
University of California, San Diego, La Jolla, California 92093-0356

(Received 31 January 2005; accepted 1 June 2005)

We have measured the rovibronic densities of four symmetric (C_{2v}) and two asymmetric (C_s) isotopologues of nitrogen dioxide just below their photodissociation threshold. At dissociation threshold and under jet conditions the laser-induced fluorescence abruptly disappears because the dissociation into $NO(^2\Pi_{1/2})+O(^3P_2)$ is much faster than the radiative decay. As a consequence, in a narrow energy range below D_0, the highest bound rovibronic energy levels of $J=1/2$ and $J=3/2$ can be observed and sorted. A statistical analysis of the corresponding rovibronic density, energy spacing, and rovibronic transition intensities has been made. The observed intensity distributions are in agreement with the Porter-Thomas distribution. This distribution allows one to estimate the number of missing levels, and therefore to determine and compare the rovibronic and the vibronic densities. The four symmetric NO_2 isotopologues, $^{16}O^{14}N^{16}O$, $^{18}O^{14}N^{18}O$, $^{16}O^{15}N^{16}O$, and $^{18}O^{15}N^{18}O$, have, respectively, a sum of $J=1/2$ and $J=3/2$ rovibronic densities of 18 ± 0.8, 18.3 ± 1.4, 18.4 ± 2.7, and $19.8\pm3.5/cm^{-1}$, while for the two asymmetric isotopologues, $^{18}O^{14}N^{16}O$ and $^{18}O^{15}N^{16}O$, the corresponding densities are 20.9 ± 4.5 and $23.6\pm5.6/cm^{-1}$. The corresponding vibronic densities are in agreement only if we include both the merging of symmetry species (from those of C_{2v} to those of C_s) and the contribution of the long-range tail(s) of the potential-energy surface along the dissociation coordinate. The effects of isotopic substitution on dissociation rates and the possible relation to mass-independent isotopic fractionation are discussed. © *2005 American Institute of Physics*. [DOI: 10.1063/1.1978873]

I. INTRODUCTION AND OBJECTIVE

During the last three decades considerable effort has been devoted to the observation and understanding of the NO_2 visible spectrum and photodissociation process.[1–16] It has been shown that the notorious complexity of the NO_2 visible spectrum is due to the conical intersection between the two low-lying $^2A_1$ and $^2B_2$ electronic states.[3,16–18] For the $^{16}O^{14}N^{16}O$ isotopologue, it has been established that the vibronic degrees of freedom are chaotic above $\approx 16\,500\ cm^{-1}$ (2 eV)[9,10,19] and that rovibronic eigenstates are chaotic above $24\,000\ cm^{-1}$ (3 eV).[6,20] This implies that the rovibronic chaos is completely developed at energies below the $^{16}O^{14}N^{16}O$ dissociation threshold located at $25\,128.56\ cm^{-1}$.[6,21] In addition, an abrupt increase of the rovibronic density has been observed in a range of $\approx 20-30\ cm^{-1}$ below D_0.[21,22] This has been interpreted in terms of a contribution of long-range interactions (dipole-quadrupole and quadrupole-quadrupole) in the tail of the potential-energy surface (PES) along the $R(NO-O)$ dissociation coordinate.[23] Resonances located just above D_0 have been measured in the frequency domain and the rates have been measured up to a large energy excess in the time domain.[11–15]

The study of the dissociation dynamics of NO_2 isotopologues is also of interest to geophysicists because its symmetry characteristics are the same as those found in ozone. There has been considerable interest in the anomalous oxygen isotope ratios (^{16}O, ^{17}O, and ^{18}O) observed in stratospheric ozone and other oxygenated molecules such as CO_2 and sulfate and nitrate contained in aerosols.[24–27] There are also unexpected oxygen isotope ratios observed in meteorites,[28,29] which have been linked to solar system formation processes. These unconventional oxygen isotope ratios are globally classified as "mass-independent fractionations" (MIF)[27] because ^{17}O and ^{18}O are equally enriched (depleted), where statistical mechanics predicts ^{18}O enrichment (or depletion) should be about twice that of ^{17}O (e.g., the fractionations appear to be independent of the isotope's relative mass differences). The most studied MIF system occurs in the formation of ozone,[27,30–32] which has led to a variety of theoretical models that invoked the symmetry differences between isotopically substituted and unsubstituted molecules.[33–37] Ozone is a C_{2v} triatomic molecule when the two terminal oxygen atoms are identical, but whose symmetry is reduced to C_s when the two terminal oxygen atoms are different. Mauersberger *et al.*[32,38] have shown that ozone formed by photolysis, occurring in O_2 mixtures enriched in ^{17}O and ^{18}O, produces isotopologues with nonstatistical dis-

[a]Electronic mail: gmichalski@ucsd.edu

tributions, with formation of the asymmetric isotopologues (C_s) being favored over the symmetric (C_{2v}). Grebenshchikov *et al.* have also shown that the barrier height to isotopic exchange between the central oxygen atom with one of the two terminal atoms is too high to be overcome by collisional processes.[39]

Each theoretical model, including the two most recent by Hawthorn *et al.*[33,34] and by Robert and Camy-Peyre,[37] presupposes that the formation and/or dissociation rates for C_{2v} and C_s isotopologues are different, and incorporate this difference using a dimensionless factor based on the experimentally observed rate differences.[32] The first-principle nature of this empirical factor is still unclear, i.e., what is the underlying physics that causes symmetric and asymmetric isotopologues O_3 to have such different rates of formation? Further, does this also apply to other molecules whose symmetry can be reduced by isotopic substitution such as triatomic molecules of the $^xOA^yO$ type (such as SO_2, NO_2,…) with $x,y=16,17,18$, regardless of the elemental makeup of the central atom (A)? MIF may also occur in larger molecules such as the nitrate radical whose symmetry is also reduced by isotopic substitution. The dimensionless correction factor may be related to the differences in the zero-point energy (ZPE)[40,41] and/or strictly to the symmetry dependence of the rates of formation and dissociation due to unequal density of states in C_{2v} and C_s molecules.[33,34] There have been no direct experimental tests for the validity of these hypotheses.

In contrast to O_3, the NO_2 photodissociation at threshold can be experimentally studied in detail. Although resonances have been observed above D_0, this paper is only concerned with the bound states, just below D_0, of the four symmetric (C_{2v}) and two asymmetric (C_s) isotopologues of NO_2 (isotopologues containing ^{17}O were not analyzed). It is important to realize that symmetric isotopologues ($^xON^xO$) have a single (degenerate) dissociation channel ($N^xO+{}^xO$) while asymmetric isotopologues, $^xON^yO$, have two different dissociation channels ($N^yO+{}^xO$ and $N^xO+{}^yO$) with different D_0 values because the ZPE of both $N^{x,y}O$ products and parent NO_2 isotopologues are different.[42] The second property which may be expected to be different for asymmetric versus symmetric isotopologues is the average photodissociation (and/or formation) rate. According to Rice-Ramsperger-Kassel-Marcus (RRKM) theory, these rates depend on the density of states for dissociation and formation. Through some symmetry dependence of the selection (or propensity) rules, it may be possible to have different state densities for the C_{2v} relative to the C_s isotopologues, resulting in different rates and hence the evolution of the MIF effect (since symmetry can be equally broken by either ^{17}O or ^{18}O).

Recently, we have measured the D_0 of six NO_2 isotopologues (four symmetric and two asymmetric),[42] which can be expressed as the sum of a single $D_e(26\,051.17\pm0.7\ \mathrm{cm}^{-1})$ plus the ZPE of the parent NO_2 minus the ZPE of the NO product(s). Experimentally, these six D_0 corresponded to the laser energy for which the laser induced fluorescence (LIF) is abruptly discontinued. The LIF spectra permit one to determine the sum of the $J=1/2$ and $J=3/2$ level densities and to study the corresponding statistical properties for each NO_2 isotopologue.

This paper is based on the statistical analysis of the $J=1/2$ and $J=3/2$ rovibronic levels located in the vicinity of the dissociation threshold and of the corresponding transition intensities. This analysis of the rovibronic properties of NO_2 near D_0 has been performed in order to predict isotope substitution effects on unimolecular rates applying the RRKM rate formula.

II. EXPERIMENT

The experimental apparatus and conditions have been previously described.[20,42] In short, a monomode laser beam excites the NO_2 molecules in the cold region of a supersonic jet expansion. The LIF is detected with a photomultiplier perpendicular to the jet axis and to the laser beam. Two critical parameters for the results presented here are the S/N ratio (which is higher than 10^{+3} for the $^{16}O^{14}N^{16}O$ isotopologue) and the spectral resolution. Our resolution of about 250 MHz is limited by the residual Doppler effect and can partially resolve the hyperfine splitting (221 MHz) of the initial $N=0$, $K=0$, and $J=1/2$ level, which is dominantly populated in the jet expansion. Near D_0, the resolution of 250 MHz is about one tenth of the mean spacing between R_0 lines for each isotopologue so the fraction of unresolved lines is negligible. Difficulties arise when one or more isotopologues are present in the gas mixture. We have been unable to isolate pure asymmetric isotopologues because of the scrambling of oxygen atoms in gas-phase NO_2 via the transient formation of the N_2O_4 dimers,[43] which produces a statistical mixture of symmetric and asymmetric isotopologues. To help resolve the spectral interference between isotopologues we have recorded LIF spectra with various ratios of ^{16}O and ^{18}O (and then of $^{16}O^{14}N^{16}O$, $^{18}O^{14}N^{16}O$, and $^{18}O^{14}N^{18}O$ isotopologues) in order to use the relative intensities as a criterion to assign each line to a given isotopologue. Additional details on assigning fluorescence lines to their respective isotopologue in mixed gases can be found elsewhere.[42] For the sake of compactness the isotopologues are noted (646) for $^{16}O^{14}N^{16}O$, (846) for $^{18}O^{14}N^{16}O$, and so on.

III. RESULTS

A. Rovibronic level counting ($J=1/2$ and $3/2$) for symmetric NO_2 isotopologues

For each symmetric isotopologue we have obtained a list of R_0 lines, (and the $J=1/2$ and $J=3/2$ rovibronic energy levels) observed by LIF in the range from (D_0-6B) to D_0. The D_0 values are the photodissociation thresholds, which are unique to each isotopologue and have previously been determined.[42] The rotational constants B are also unique for each isotopologue. The range of $6B$ corresponds to the energy difference between $N=0$ and $N=2$ of the $K=0$ stack in the (0,0,0) ground state. The values of $6B$, from 2.53 cm^{-1} (646) to 2.25 cm^{-1} (858) are given in Table III. In the range from (D_0-6B) to D_0 only R_0 transitions are observed by LIF because all other allowed transitions, P_2, R_2, P_4, R_4, etc. of the $K=0$ stack and those of the $K\geqslant 1$ stacks, reach upper levels which are above D_0. These upper levels are resonances with a lifetime of the order of 100 ps or less, about four orders of magnitude shorter than the radiative lifetime of the

TABLE I. $J=1/2$ and $3/2$ rovibronic symmetries for NO_2 isotopologues of C_{2v} and C_s symmetries. The levels observed by LIF are in bold. The missing levels are in brackets. This table does not include the contributions of the B^2B_1 and C^2A_2 electronic states which are assumed to be negligible. This is why the two columns corresponding to $\Gamma_{vib}:A_2$ and $\Gamma_{vib}:B_1$ are missing for the C_{2v} symmetry. For the C_s symmetry, the column $\Gamma_{vib}:A''$ would have been omitted because all the rovibronic levels belong to A'' electronic states which are the C_s counterpart of the B^2B_1 and C^2A_2 electronic states observed for the C_{2v} (646) isotopologue.

		C_{2v} symmetry			C_s symmetry		
			Γ_{rovib}			Γ_{rovib}	
K,N and Ka,Kc	J	Γ_{rot}	$\Gamma_{vib}:A_1$	$\Gamma_{vib}:B_2$	Γ_{rot}	$\Gamma_{vib}:A'$	$\Gamma_{vib}:A''$
$K=0,N=0$,ee	$J=1/2$	A_1	A_1	(B_2)	A'	A'	A''
$K=0,N=1$,eo	**$J=1/2$**	B_1	(B_1)	**A_2**	A''	**A''**	A'
$K=0,N=1$,eo	**$J=3/2$**	B_1	(B_1)	**A_2**	A''	**A''**	A'
$K=0,N=2$,ee	$J=3/2$	A_1	A_1	(B_2)	A'	A'	A''
$K=1,N=1$,oo	**$J=1/2$**	A_2	**A_2**	(B_1)	A''	**A''**	A'
$K=1,N=1$,oo	**$J=3/2$**	A_2	**A_2**	(B_1)	A''	**A''**	A'
$K=1,N=1$,oe	$J=1/2$	B_2	(B_2)	A_1	A'	A'	A''
$K=1,N=1$,oe	$J=3/2$	B_2	(B_2)	A_1	A'	A'	A''
$K=1,N=2$,oo	**$J=3/2$**	A_2	**A_2**	(B_1)	A''	**A''**	A'
$K=1,N=2$,oe	$J=3/2$	B_2	(B_2)	A_1	A'	A'	A''
$K=2,N=2$,ee	$J=3/2$	A_1	A_1	(B_2)	A'	A'	A''
$K=2,N=2$,eo	**$J=3/2$**	B_1	(B_1)	**A_2**	A''	**A''**	A'

bound levels located below D_0. Such an abrupt change in the lifetime is due to the absence of barrier along the dissociation coordinate. For higher J, we expect a significant rotational barrier but this barrier (which can be roughly estimated to be less than 10^{-2} cm^{-1} for the $N=1$; $K=0$ and $K=1$ or $N=2$; $K=2$ levels of interest, see below) is much smaller than the average level spacing that is of the order of 0.05 cm^{-1}. As a result, only R_0 transitions give a detectable LIF signal in the energy range of $6B$ ($\sim$2.5 cm^{-1}) below D_0.

In order to analyze the observed line density, which is the sum of $J=1/2$ and $J=3/2$ level densities, it should be noted that a strong rovibronic mixing exists. This means that all levels of the same J and the same overall rovibronic symmetry are strongly mixed and that they share the bright character of the zero-order rovibronic levels. This has been demonstrated previously by an extensive statistical analysis of about 1700 rovibronic transitions in the main (646) isotopologue.[10,20]

According to the optical selection rules for NO_2,[44] when the $A^2B_2 \leftarrow X^2A_1$ parallel ($\Delta K=0$) electronic transition is considered, for each upper vibronic level of B_2 symmetry (noted $\Gamma_{vib}:B_2$), there is only one zero-order rotational bright level, $N=1$, $K=0$, which can be reached by a R_0 transition from the $N=0$, $K=0$ ($J=1/2$) rotational level. Each $N=1$, $K=0$ level is of an A_2 overall rovibronic symmetry and is split into two fine-structure components of $J=1/2$ and $J=3/2$. The effect of the rovibronic interactions[20] is to mix each of these two bright levels with other rovibronic levels of the same J, $J=1/2$ or $J=3/2$, and the same A_2 overall rovibronic symmetry. The $N=1$, $K=0$ of each upper $\Gamma_{vib}:B_2$ has four levels of this "dark" type: one with $\Gamma_{vib}:B_2$, $N=2$, $K=2$, $J=3/2$, and three with $\Gamma_{vib}:A_1$, $N=1$, $K=1$, $J=1/2$ and $J=3/2$ and $N=2$, $K=1$, $J=3/2$. Table I summarizes the vibronic and rovibronic symmetries of all states, both for C_{2v} and C_s isotopologues. Calculations have shown that the $\Gamma_{vib}:B_2$ and the $\Gamma_{vib}:A_1$ vibronic densities are almost the same when $E \approx D_0$.[45] This means that, for each level of $\Gamma_{vib}:B_2$, there are one $N=1$, $K=0$ bright level (which is split into one $J=1/2$ and one $J=3/2$) and, statistically, four dark levels as listed above. Together, we expect six levels, i.e., up to 6 R_0 transitions per bright vibronic level of $\Gamma_{vib}:B_2$ when rovibronic mixing is strong enough to allow all the corresponding transitions to be observed.

These six R_0 transitions should be compared with the two R_0 transitions (one $J=1/2$ and one $J=3/2$) per B_2 vibronic level expected in the absence of rovibronic interaction. The 6/2 ratio is important to recover the vibronic density of states from the observed density of R_0 rovibronic transitions. Note that the 6/2 ratio applies only for R_0 transitions, this ratio being slightly different for transitions from higher J values, which are not considered here.[20] The strong rovibronic mixing regime has been shown to be statistically valid by the analysis of about 1500 rovibronic transitions (R_0, P_2, R_2, P_4, R_4) of the (646) isotopologue observed around 2.9 eV.[20] The key argument is the observed 1/2 (in fact, 2/4) ratio between the $J=1/2$ and $J=3/2$ densities of R_0 transitions while a 1/1 ratio is expected (and observed at low energies) when rovibronic mixing is negligible. All previous results support strong rovibronic mixings (or rovibronic chaos) in the "blue" part of the NO_2 spectrum above 3 eV, i.e., near D_0. Rovibronic chaos can also be tested by the next neighbor distribution (NND) which, for chaotic regime, display the well-known "level repulsion" and which is well described by the semiempirical Wigner distribution.[44] However, the NND analysis requires a pure, long, and almost complete sequence of levels of the same J value. These conditions are difficult to fulfill simultaneously. However, these conditions are almost met in the narrow range of $6B$ below D_0. Chaos can also be tested with the distribution of line intensities, which is a Porter-Thomas law for chaotic systems

TABLE II. Summary of the R_0 lines counting for the six NO_2 isotopologues (see text).

Isotopologue	Number of observed R_0 lines	Z_{cut}	m	Number of missing R_0 lines	Total number of R_0 lines
646	42	0.01	0.079	3.6	45.6±2
848	36	0.03	0.125	5.1	41.1±3
858	29	0.15	0.3	12.5	41.5±6
656	32	0.22	0.36	18	50±8
846	12	0.17	0.32	5.6	17.6±4
856	13	0.24	0.375	7.8	20.8±5

of Gaussian orthogonal ensemble (GOE) type. Other statistics like Δ_3 and Σ^2 cannot be used here because our four sets of levels are limited.

We also note that the degree of rovibronic mixing depends only on the potential-energy surfaces of the two electronic states, which in the Born-Oppenheimer approximation is the same for each isotopologue. Therefore, although there may be some small uncertainty in the precise proportions of dark and bright states, these uncertainties cancel when comparing the *relative* number of states between isotopologues.

1. Intensity distributions

In order to determine the true rovibronic density it is necessary to analyze the intensity distribution of R_0 lines. Once the Porter-Thomas distribution is reasonably established, it is possible to estimate the number of weak (and then missing) lines because of our finite S/N ratio. The results and the analysis of 42 R_0 transitions observed between $D_0=25\,128.56\ cm^{-1}$ and $D_0=-2.532\ cm^{-1}$ for the 646 isotopologue have already been published.[20] The set of 42 R_0 line intensities follows the Porter-Thomas distribution over more than three orders of magnitude of z, the normalized intensities $z_i=I_i/\langle I\rangle$, where $\langle I\rangle$ is the average intensity. The Porter-Thomas normalized distribution is given by $P(z)=(2\pi z)^{-1/2}\exp(-z)$. Therefore, the true $\langle I\rangle$ value requires knowledge of the number of missing lines, which correspond to the weak intensities between $z=0$ and z_{cut}, where z_{cut} corresponds to our limit of detection ($S/N>1$). Then, assuming that the Porter-Thomas remains valid for very low intensities (between $z=0$ and z_{cut}), we can estimate the number of missing transitions (and then the missing levels). As a consequence, knowing z_{cut}, the minimum detectable value of z that corresponds to the normalized intensity of the weakest detectable line, it is possible to calculate m, the fraction of missing levels, $m=\int_0^{z_{cut}}P(z)dz=\mathrm{erf}((z_{cut}/2)^{1/2})$. With $z_{cut}=0.01$, which corresponds to our S/N ratio of $\approx 10^{+3}$ for the 646 isotopologue, we obtained $m=0.08$. From this value, the total number of R_0 lines can be estimated: $N_t(646)=42/(1-m)=45.6$ lines over $2.53\ cm^{-1}$. This corrected number should be used to renormalize the $\langle I\rangle$ and then the corresponding z. Formally, this procedure gives a new z_{cut}, but a convergence is obtained after typically one or two iterations. An uncertainty of ±2 lines can be estimated from the expected (nonstatistical) fluctuations. It is important to notice that these fluctuations are significantly reduced for a chaotic system compared to a random distribution.[46]

The same procedure has been used to analyze the LIF of three other symmetric isotopologues. The S/N ratios of these three LIF spectra are weaker than for (646) because, due to reagent expense, the mixture of the rare isotope NO_2 with He contained an order of magnitude less NO_2 than the (646) mixture. This leads to a larger z_{cut}, larger m values, and to a higher fraction of missing R_0 lines (levels). The z_{cut} and m values and the corrected numbers of lines are summarized in Table II for the four symmetric isotopologues. In Fig. 2, a visual inspection and a comparison of the four observed histograms with the Porter-Thomas[44] distribution indicates an overall reasonable agreement.

2. Next neighbor distribution (NND)

A second aspect of our analysis concerns rovibronic energy spacings, i.e., the next neighbor distribution (NND). The NND is obtained from the dimensionless normalized energy spacings S such that $\langle S\rangle=1$. The NND of the set of 42 levels of the (646) isotopologue have already been published.[21] If the NO_2 rovibronic levels are fully chaotic close to D_0, the NND distributions for $J=1/2$ solely and for $J=3/2$ solely are expected to be Wigner distributions. However, we are unable to discriminate the $J=1/2$ and $J=3/2$. Instead, the set of R_0 lines is a random superposition of the subset of $J=1/2$ levels (weight=2/6) and of the subset of $J=3/2$ levels (weight of 4/6). The weights are derived from Table I, assuming the same A_1 and B_2 vibronic densities. We have previously calculated the NND expected for the random superposition of two subsets of weight 1/3 and 2/3 having individually a NND of Wigner type.[21] The well-known "level repulsion" is only partially washed out near the origin as shown on Fig. 3. The level repulsion can also be characterized by σ, the standard deviation of the normalized distribution of spacing. For a random set of levels (Poisson distribution), $\sigma=1$ while for a Wigner distribution $\sigma=0.53$. For a random superposition of two subsets of relative weight of 1/3 and 2/3, which obey individually a Wigner distribution, we expect a normalized standard deviation of $\sigma=0.68$.[18] The values of σ for the four symmetric isotopologues are 0.665 for (646), 0.618 for (848), 0.55 for (858), and 0.53 for (656). The two last values are very rough because of the large fraction of missing levels (large m, see above) and can be discarded. Globally, the NNDs of the four symmetric isotopologues agree with a strong rovibronic mixing near the dissociation threshold, at least for the low J values considered here.

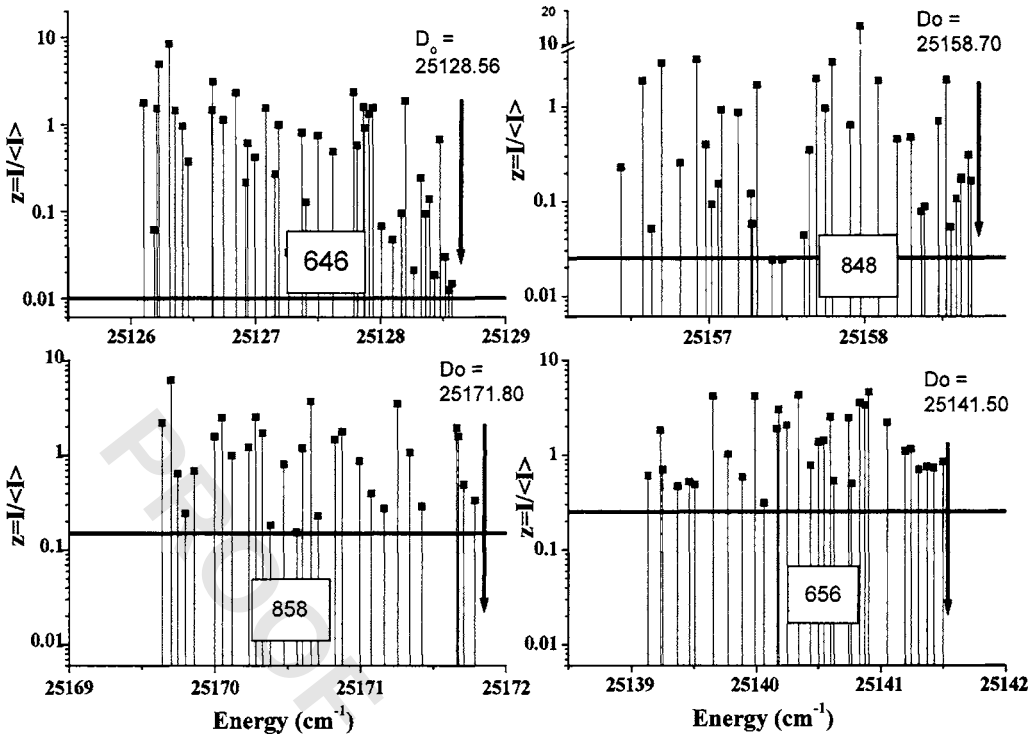

FIG. 1. Stick spectra of the four symmetric isotopologues in their D_0-6B to D_0 energy range. The intensities are normalized to an average value of 1. A log scale is used for the intensities because they range over nearly to three orders of magnitude. The limit of detection (or detection threshold) of each isotopologue is represented.

3. Rovibronic and vibronic densities of symmetric isotopologues

For each symmetric isotopologue (yxy), the expected numbers of R_0 lines, $Nt(yxy)$ (which are the expected numbers of $J=1/2$ and $J=3/2$ levels, see Sec. III A 1) have been used to determine the sum of $J=1/2$ and $J=3/2$ level densities just below D_0. We first derive these densities by dividing the $Nt(xyx)$ given in Table II by the corresponding en-

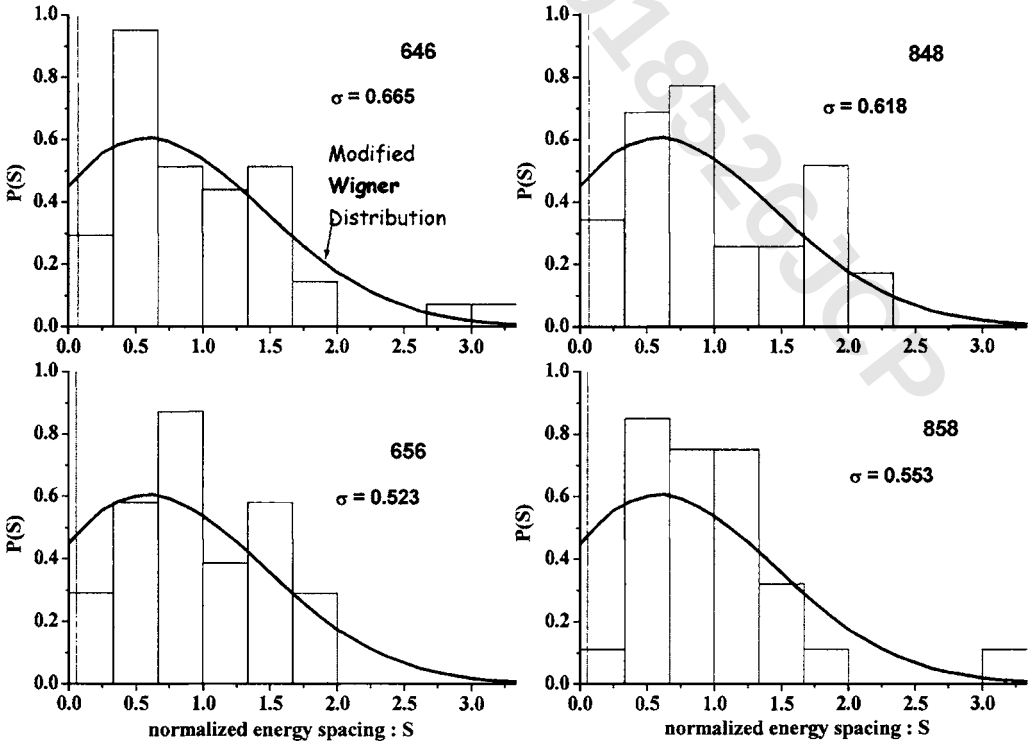

FIG. 2. Histograms of the intensities in a standard log-log plot (Ref. 44). The widths of the bins are in a progression of $\sqrt{10}$. The continuous curve is the Porter-Thomas distribution (Ref. 44) (see text). For each isotopologue, we give the number of observed R_0 transitions and the number of R_0 transitions (Nt) expected if the Porter-Thomas distribution remains valid for the (missing) weak transitions (see Table II).

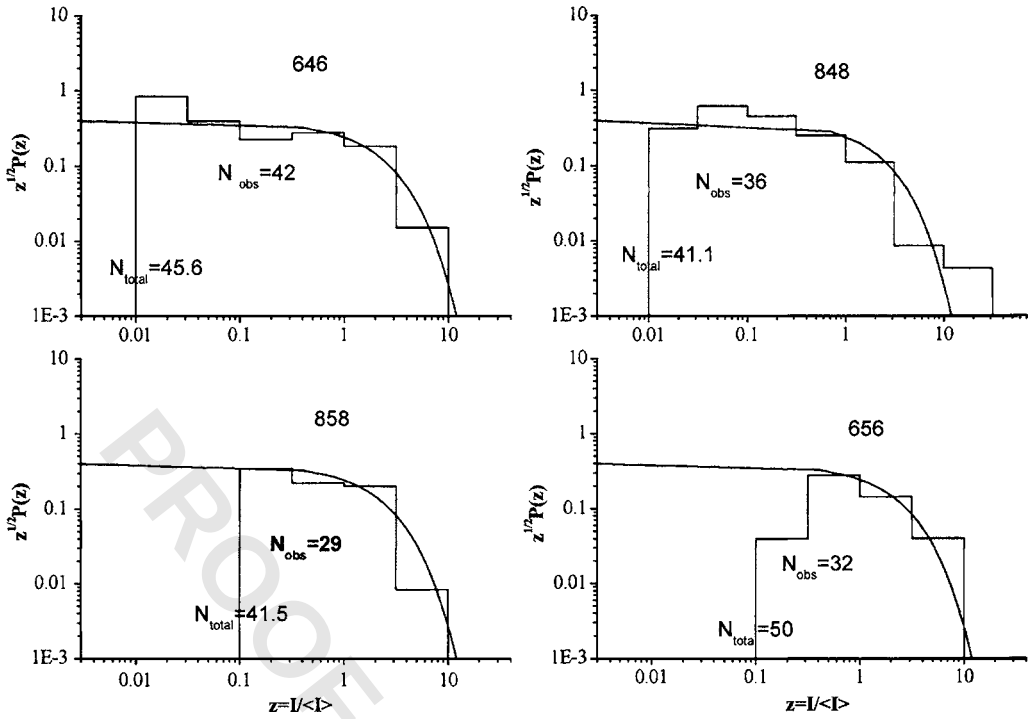

FIG. 3. The next neighbor distribution (NND) for the four symmetric isotopologues. The smooth curve is a modified version of the Wigner distribution which apply for the random superposition of two subsets of weight 2/3 and 1/3, which correspond to $J=3/2$ and 1/2 and which obey individually to the Wigner distribution (see text). The standard deviation σ is expected to be 0.68 instead of 0.53 for a single set of level obeying a Wigner distribution. The experimental resolution, which corresponds to 0.07 average spacing for (646), is represented by a vertical dashed line in the first bin.

ergy range of $6B$ for symmetric isotopologues. The corresponding rovibronic level densities, ρ_{rovib} ($J=1/2$ and $J=3/2$; A_2) where A_2 stands for the overall rovibronic symmetry, are compared in Table III. The PES being the same for all the isotopologues within the Born-Oppenheimer (BO) approximation, only two minor effects have to be considered if we compare the rovibronic densities of the four symmetric isotopologues. The first and dominant effect is the variation of the vibrational frequencies. More precisely, the leading term in the density formula[45] is proportional to the inverse of the product of the three harmonic frequencies. Taking the rovibronic density of the (646) isotopologue as a reference, we can approximately predict the rovibronic density of a symmetric isotopologue (xyx) as

$$\rho_{\text{rovib}}(xyx;J=1/2 \text{ and } J=3/2;A_2) = R^*_{xyx/646}\rho_{\text{rovib}}(646;J=1/2 \text{ and } J=3/2;A_2), \quad (1)$$

where $R_{xyx/646}$ are the ratios of the inverse product of three vibrational frequencies of the rare symmetric isotopologue (ω^*) relative to 646:

$$R_{xyx/646} = \omega_1\omega_2\omega_3/\omega^*_1\omega^*_2\omega^*_3. \quad (2)$$

The ratios $R_{xyx/646}$ for $(xyx)=(848)$, (858), and (656) are given in Table III. The second effect, which has been neglected, is because the rovibronic state densities at D_0 is a function of total energy taken from the zero-point energy, which are different for each isotopologues as determined by their different D_0's.

The observed rovibronic densities divided by the corresponding $R_{xyx/646}$ are expected to be the same for the four symmetric isotopologues. These normalized rovibronic densities given in the last column of Table III are equal within the error bars of 10%–15% as expected. This leads us to derive a weighted average rovibronic density of $17.4\pm0.6/\text{cm}^{-1}$, which is normalized on the (646) isotopologue. Conversely, the $R_{xyx/646}$ ratios should be taken into

TABLE III. Comparison of the sum of $J=1/2$ and $J=3/2$ rovibronic densities for six isotopologues of NO_2 near D_0.

Isotopologue	Total number of R_0 lines	ΔE^a (cm^{-1})	ρ_{rovibro} (per cm^{-1})	Ratio: $R_{xyx/646}$	ρ_{rovibro} (per cm^{-1}) $R_{xyx/646}$
646	45.6±2	2.532	18.0±0.8	1 (def)	18.0±0.8
848	41.1±3	2.256	18.3±1.4	1.1	16.5±1.3
858	41.5±6	2.25	18.4±2.7	1.15	16.0±2.2
656	50±8	2.52	19.8±3.5	1.05	18.9±3.2
846	17.6±4	0.8	22.0±4.6[b]	1.05	20.9±4.5[b]
856	20.8±5[b]	0.8	26.0±6.2[b]	1.1	23.6±5.6[b]

[a]Some of these values are obtained or derived from Ref. 47.
[b]These values should not be compared directly with the densities of the four symmetric isotopologues (see text).

account to predict the vibronic and the rovibronic densities of other isotopologues from the $17.4\pm0.6/\mathrm{cm}^{-1}$ value. Now, we want to derive the corresponding vibronic densities. As explained above, due to the strong rovibronic couplings, the observed rovibronic densities are related to the "true" vibronic densities according to

$$\rho_{\mathrm{rovib}}(xyx;E=D_0;\Gamma_{\mathrm{rovib}};A_2) = 3^*\rho_{\mathrm{vib}}(xyx;E=D_0;\Gamma_{\mathrm{vib}}:B_2) + 3^*\rho_{\mathrm{vib}}(xyx;E=D_0;\Gamma_{\mathrm{vib}}:A_1). \quad (3)$$

The two factors of 3 are the numbers of rovibronic levels of the proper A_2 rovibronic symmetry derived for $\Gamma_{\mathrm{vib}}:B_2$ and $\Gamma_{\mathrm{vib}}:A_1$ in Table I. Near D_0, the A_1 and B_2 vibronic densities are almost equal[44] and then the rovibronic densities is given by

$$\rho_{\mathrm{rovib}}(xyx;E=D_0;\Gamma_{\mathrm{rovib}}:A_2) \cong 6^*\rho_{\mathrm{vib}}(xyx;E=D_0;\Gamma_{\mathrm{vib}}:A_1(\mathrm{or}\ B_2)) \quad (4)$$

or

$$\rho_{\mathrm{rovib}}(xyx;E=D_0;\Gamma_{\mathrm{rovib}}:A_2) \cong 3^*\rho_{\mathrm{vib}}(xyx;E=D_0;\Gamma_{\mathrm{vib}}:A_1+B_2). \quad (5)$$

From the average $\rho_{\mathrm{rovib}}(646;E=D_0;\Gamma_{\mathrm{rovib}}:A_2)=17.4\pm0.6\ \mathrm{cm}^{-1}$ we derive an average $\rho_{\mathrm{vib}}(646;E=D_0;\Gamma_{\mathrm{vib}}:A_1+B_2))=5.8\pm0.24\ \mathrm{cm}^{-1}$. This value is about six times larger than the value estimated from both measurements at lower energies and standard calculations.[43] This very rapid increase of the rovibronic densities of the symmetric isotopologues just below D_0 value is attributed to the long-range tail of the PES near D_0.[19,20] In the absence of a dissociation threshold (and then of the corresponding tail of the PES), the expected "normal" vibronic density at D_0 should be almost the same as the one expected at energy $E\cong D_0-30\ \mathrm{cm}^{-1}$ because, for a triatomic molecule, the vibrational (vibronic) density goes approximately as the square of the energy. For an increase in energy of $30\ \mathrm{cm}^{-1}$, about 0.12% of the total energy D_e, the corresponding normal density, is expected to increase by roughly 0.24%. This is in stark contrast with the experimentally observed change in the rovibronic density that is in excess of 600%.[22] This increase has been interpreted as an effect of the long-range tails of the PES along the two degenerate dissociation channels.[23] According to formula (1) of Ref. 20, the vibronic density (and then the corresponding rovibronic density) at energy E can be expressed as a sum of two-dimensional (2D) densities one-dimensional [(1D) for the $R_{(O-NO)}$ distance and 1D for the relevant angle between O and the NO axis]. Each of these 2D densities is taken at an energy E', such that the total $E=E'+E(\mathrm{NO})$ is fixed, where $E(\mathrm{NO})$ are the various vibrational energies of the NO product. At the threshold of the $NO_2 -> NO(^2\Pi_{1/2})+O(^3P_2)$ dissociation process, $E(\mathrm{NO})=\frac{1}{2}\hbar\omega_{\mathrm{NO}}$ because NO is formed only in the $v=0$ level. Therefore, at $E\cong D_0$, the three-dimensional (3D) vibronic density of NO_2 is dominated by the 2D contribution at $E'=E-\frac{1}{2}\omega_{\mathrm{NO}}$ which increases abruptly near D_0 because of the long-range tail of the PES as explained in Ref. 20.

The abrupt increase of the rovibronic density near D_0 displayed in Fig. 1 of Ref. 19 and on Figs. 2 and 3 of Ref. 20 can be empirically described as the sum of the "normal" density plus an "extra" density, which can be described as the product of the normal density by a dimensionless amplification factor $\alpha(E)$. The extra density is negligible at energies lower than $E\cong D_0-30\ \mathrm{cm}^{-1}$ and increases very rapidly with E up to D_0. A convenient, empirical, and simple analytic form for $\alpha(E)$ is

$$\alpha(E)=\alpha_0\exp(-(D_0-E)/\delta) \quad (6)$$

with $\delta\approx10\ \mathrm{cm}^{-1}$. Note that this expression is valid only for $E<D_0$ and is expected to be valid for all the symmetric isotopologues because they have the same PES. The same amplification factor also applies to the vibronic densities near the threshold. This leads to the relation between the normal vibronic density (below $D_0-30\ \mathrm{cm}^{-1}$) and the "anomalous" vibronic density between D_0-30 cm−1 and D_0:

$$\rho_{\mathrm{vib}}(xyx;E\cong D_0;\Gamma_{\mathrm{vib}}:B_2) \cong \rho_{\mathrm{vib}}(xyx;E\cong D_0-30\ \mathrm{cm}^{-1};\Gamma_{\mathrm{vib}}:B_2)^*(1+\alpha(E\cong D_0)). \quad (7)$$

The factor 1 in the parentheses on the right side accounts for the normal vibronic density (in the absence of the contribution of the long-range tail of the PES), and $\alpha(E)$ accounts for the contribution of the long-range tail of the PES. Note that there are two degenerate dissociation channels for symmetric isotopologues and only one channel when only the lowest dissociation threshold of asymmetric isotopologues is considered; this leads us to reduce the amplification parameter by a factor of two when the lowest dissociation threshold of asymmetric isotopologues is considered (see below). This formula is also valid when $\Gamma_{\mathrm{vib}}:A_1$ and thus for the sum of the two, $\Gamma_{\mathrm{vib}}:A_1+B_2$. At energies slightly lower than $\cong D_0-30\ \mathrm{cm}^{-1}$ the measured B_2 vibronic density[19,20] is $\rho_{\mathrm{vib}}(646;E\cong D_0-30\ \mathrm{cm}^{-1};\Gamma_{\mathrm{vib}}:B_2))=0.5\pm0.05\ /\mathrm{cm}^{-1}$, in agreement with various types of density calculations[4,45,47] and measurements.[8,17,43] From the observed rovibronic density of Table III, we derive the observed vibronic density at D_0: $\rho_{\mathrm{vib}}(646;E\cong D_0;\Gamma_{\mathrm{vib}}:B_2)=3\pm0.13\ /\mathrm{cm}^{-1}$ according to formula (4). This density is in stark contrast with the expected density of $0.5\pm0.05\ /\mathrm{cm}^{-1}$. From the ratio of the two and according to formula (7), we determine the dimensionless factor $(1+\alpha(E=D_0))=(1+\alpha_0)=6\pm0.8$ and, from this, $\alpha_0=5\pm0.8$. If we use the average rovibronic density of $17.4\pm0.6\ /\mathrm{cm}^{-1}$ (see above) we derive $\alpha_0=4.8\pm0.6$, which is an average for the four symmetric isotopologues. Above we approximate $\alpha(E)$ to α_0 over the range of D_0-6B up to D_0, if we take the energy dependence of $\alpha(E)$ into account [see (6)] we find $\alpha_0=5.4\pm0.6$.

The conclusion that all symmetric NO_2 isotopologues have the same rovibronic and vibronic densities is important because we desire to make a relevant comparison with the same densities in the asymmetric isotopologues (see below Sec. III B). It has been established by several groups that the NO_2 dissociation follows RRKM like behavior[48,11,15,49] but random fluctuation in the density are also observed over nar-

row energy ranges. Although the large and abrupt increase in the rovibronic density just below D_0 has been attributed to the dipole-dipole and dipole-quadrapole interaction in the long-range tail of the PES, a random fluctuation near D_0 cannot *a priori* be ruled out. In a chaotic system the probability that each symmetric isotopologues exhibits such a large density fluctuation near D_0 is negligible and therefore, the rovibronic density increase is likely due to the shape of the PES just below D_0. The good agreement between the rovibronic densities over the $6B$ energy range below D_0 for each isotopologue ensures that our comparisons of densities are over a sufficiently large energy range. In Sec. III B we apply the same method of analysis and the same assumptions, such as the Porter-Thomas intensity distribution, for the analysis of asymmetric isotopologues. Our goal is to make a *relative* comparison of densities and then of RRKM rates and not an absolute determination of these distributions. The previous work on the more abundant 646 isotopologue remains the best since the spectroscopic data is more complete and robust.

B. Asymmetric isotopologues

Statistical parity between the symmetric isotopologues and the two asymmetric isotopologues (856, 846), based on the latter's LIF spectrum, cannot be achieved for two reasons. First, as explained in the experimental section, the oxygen scrambling transforms an initial gas of (846) isotopologue into a statistical mixture of (846), (646), and (848) isotopologues.[43] This means that the three spectra superimpose and some of the lines are blended. However, by utilizing high precision on the energy scale and by varying the relative concentration of ^{16}O and ^{18}O, it is possible to extract the lines of asymmetric isotopologues from the mixed spectra. However, this method is not tractable for the very weak transitions that may be "hidden" by strong lines of the other isotopologues. A second limitation is due to the narrow energy range where only R_0 lines are present: for the asymmetric isotopologue this range is reduced to only $2B$ (from D_0-2B to D_0). The range is limited to $2B$ because both even and odd N rotational quantum numbers exist for the asymmetric isotopologues while only odd N exists in the $A\,^2B_2$ state of the $K=0$ stack of symmetric isotopologues. The range of $2B$, which is three times smaller than the range of $6B$ for symmetric isotopologues, is a severe limitation in terms of statistics. In other words, there are additional bound-bound R_1 transitions in the energy range from D_0-6B to D_0-2B of asymmetric isotopologues, which superimpose with the R_0 lines of interest. The analysis of the energy range, where R_0 and R_1 lines are present, gives too imprecise results because of spectral congestion (see above).

For these two reasons only limited results can be obtained for the (846) and (856) asymmetric isotopologues. For the (846) isotopologue, 12 R_0 lines have been observed between 25 130.12 (D_0-2B) and 25 130.92 cm^{-1} [D_0 of the (846) isotopologue].[1] The normalized intensities (such that $\langle I\rangle=1$, see above) range from 4.9 to 0.11. Assuming that the intensities follow the Porter-Thomas distribution (as for the symmetric isotopologues, see above) these intensities gives a $z_{cut}=0.17$, then $m=0.32$ from which the expected total number of about 17.6 ± 4 R_0 lines can be derived (see Table II). Taking into account the range of $2B=0.8$ cm^{-1}, a rovibronic density of 20.9 ± 4.5 lines/cm^{-1} is obtained. The corresponding results for (856) are given in Tables II and III. Again, note that the error bars do not obey the standard Poison statistics (square-root type) but rather the GOE statistics (log type) that is characterized by lower fluctuations.[45]

It is interesting to compare the rovibronic and vibronic densities of the symmetric and the asymmetric isotopologues at energies just below D_0. For asymmetric (C_s) isotopologues, the rovibronic level density of $J=1/2$ and $3/2$ with rovibronic symmetry $\Gamma_{rovib}:A''$ is given by

$$\rho_{rovib}(xyz;E\cong D_0;J=1/2 \text{ and } J=3/2;\Gamma_{rovib}:A'') = 6^*\rho_{vib}(xyz;E\cong D_0;\Gamma_{vib}:A'). \quad (8)$$

This formula is the counterpart for asymmetric isotopologues of formulas (3)–(5) which are valid for symmetric isotopologues near D_0. Note that A_1 and B_2 species in C_{2v} symmetry [see formula (5)] merge into A' species in the C_s symmetry [see formula (8)]. This allows a direct comparison of densities as discussed in the Sec. IV. The factor of 6 is the number of $J=1/2$ and $J=3/2$ levels of A'' rovibronic symmetry derived from rovibronic level counting in Table I. Again, as for symmetric isotopologues, this counting is meaningful if we assume a complete rovibronic mixing. From the rovibronic densities of 20.9 ± 4.5 and 23.6 ± 5.6 lines/cm^{-1} measured for the (846) and (856) (see Table II), we derive the vibronic density according to (8): $\rho_{vib}(846;E\cong D_0,\Gamma_{vib}:A') = 3.50\pm0.75$ cm^{-1} and $\rho_{vib}(856;E\cong D_0,\Gamma_{vib}:A') = 3.93\pm0.9$ cm^{-1}.

IV. COMPARISON OF VIBRONIC DENSITY BETWEEN SYMMETRIC AND ASYMMETRIC ISOTOPOLOGUES

We first consider energies significantly below the dissociation threshold ($E\cong D_0-30$ cm^{-1}) and assess the vibronic densities, which are not effected by the tails of the PES along the dissociation coordinate. Although we do not have any direct measurement of the rovibronic density for the asymmetric isotopologues at energies significantly lower than the threshold, we can make a good estimate if we assume that the PES are the same for all the isotopologues. This allows us to estimate the ratios of vibronic densities based on the vibrational frequencies as explained above [see formula (2)]. However, as A_1 and B_2 species of the C_{2v} group symmetry merge into the A' species of the C_s group symmetry, we estimate $\rho_{vib}(xyz;E\cong D_0-30\ cm^{-1};\Gamma_{vib}:A')$ using $\rho_{vib}(646;E\cong D_0-30\ cm^{-1};\Gamma_{vib}:A_1+B_2)$:

$$\rho_{vib}(xyz;E\cong D_0-30\ cm^{-1};\Gamma_{vib}:A') = R^*_{xyz/646}\rho_{vib}(646;E\cong D_0-30\ cm^{-1};\Gamma_{vib}:A_1+B_2). \quad (9)$$

Note that the various D_0 energies are not exactly the same but their differences can be neglected here because only the energy shift from the corresponding dissociation energy (e.g., 30 cm^{-1}) is important. From formula (9), using $\rho_{vib}(646;E=D_0-30\ cm^{-1};\Gamma_{vib}:A_1+B_2)=1.0\pm0.1$ cm^{-1} (see

above) and $R_{846/646}=1.05$ and $R_{856/646}=1.10$ (see Table III), we predict $\rho_{vib}(846;E\cong D_0-30\ cm^{-1};\Gamma_{vib}:A')\cong 1.05\pm0.1\ cm^{-1}$ and $\rho_{vib}(856;E\cong D_0-30\ cm^{-1};\Gamma_{vib}:A')\cong 1.1\pm0.1\ cm^{-1}$.

Consider now the vibronic densities just below the lowest dissociation threshold where the rovibronic densities of the asymmetric isotopologues have been measured. For symmetric isotopologues, two degenerate dissociation channels open up at D_0, while only one dissociation channel is available for the asymmetric isotopologues. This means that while the two long-range tails of the PES play a role for symmetric isotopologues, only one is relevant for asymmetric isotopologues at the first $D_0(D_{01})$. The second dissociation threshold (D_{02}) of asymmetric isotopologues [(846) or (856)] is typically located 25 cm^{-1} above D_{01} and its effect can be neglected at the energy of the lowest threshold. Then, the relevant amplification factor [see formula (6) above] for vibronic density near the lowest threshold of asymmetric isotopologues (C_s symmetry) is expected to be only half the factor for the symmetric isotopologues: $\alpha(xyz;E=D_0)=(1/2)\alpha(xyx;E=D_0)=2.4\pm0.3$ or 2.7 ± 0.3 if we use $\alpha(xyx;E=D_0)=5.4\pm0.6$ (see above). Consequently, for asymmetric isotopologues, formula (5) becomes

$$\rho_{vib}(xyz;E\cong D_0;\Gamma_{vib}:A') = \rho_{vib}(xyz;E\cong D_0-30\ cm^{-1};\Gamma_{vib}:A') \times(1+\alpha(xyz;E=D_0)). \quad (10)$$

Using (10) and the observed vibronic densities of 846 and 856 (see Table III) we derive $\rho_{vib}(846;E\cong D_0-30\ cm^{-1};\Gamma_{vib}:A')=1.03\pm0.35\ cm^{-1}$ and $\rho_{vib}(856;E\cong D_0-30\ cm^{-1};\Gamma_{vib}:A')=1.16\pm0.4\ cm^{-1}$, in good agreement with the expected values of 1.05 and 1.1 cm^{-1} (see above). Obviously, we also expect a second increase of the vibronic (and rovibronic) densities near the second dissociation threshold of asymmetric isotopologues but this energy range cannot be observed by LIF.

A NND analysis (see Sec. III A 2) has not been performed for asymmetric isotopologues because the two sets of energy level are too small. Globally, the rovibronic densities observed for the six isotopologues close to their dissociation threshold can be interpreted with a single and simple model which takes into account the singular behavior of the vibronic (and then the rovibronic) densities near each dissociation threshold. This is the main contribution of this paper.

V. DISCUSSION

The ratio of the measured densities of $J=1/2$ and $J=3/2$ rovibronic levels of asymmetric and symmetric isotopologues of NO_2 near their respective lowest dissociation threshold is about 1.25. This ratio has been explained with both the merging of rovibronic symmetries (from those of the C_{2v} group symmetry to the ones of the C_s group symmetry) and the effects of long-range tail of the PES just below the lowest dissociation threshold. Note that this ratio is expected to evolve with energy excess above D_0 and cannot be used to predict the ratio of dissociation rates at atmospheric temperatures. As mentioned by Toselli and Barker[50] (see their Sec. II D), no significant difference are expected between the rates of symmetric and asymmetric isotopologues far above their respective thresholds. Moreover they do not consider the branching ratio between the two dissociation channels of asymmetric isotopologues. Note that these authors consider only large energy excess above D_0, did not discuss the energy dependence of the rates near the threshold and did not take into account the energy gap between $D_{0(1)}$ and $D_{0(2)}$. If the dissociation of (846) occurs at energies between its two dissociation channels, $D_{0(1)}$ and $D_{0(2)}$ which are shifted by 25 cm^{-1} (see Ref. 1), only $^{14}N^{18}O+^{16}O$ can be formed. This means that the branching ratio goes to infinity. Experimentally, this is only true at low temperature of the order of few Kelvin. Nevertheless, a propensity remains at higher temperature and the branching ratio between the two dissociation channels is expected to deviate from unity. Therefore, when the photodissociation of a mixture of symmetric and asymmetric isotopologues is considered, both differences in dissociation rates and in branching ratio should be taken into account. We plan to consider these two aspects in the near future. Analogously, the differences between the formation rates of symmetric and asymmetric isotopologues should also be taken into account. When a mixture of ^{16}O, ^{17}O, and ^{18}O is considered, the ratios of dissociation and formation rates can either be "mass dependent" or "mass independent" (MIF type). Clearly, the effects directly linked to the differences in the zero-point energy (ZPE) of the parent NO_2 and of the NO product (e.g., the difference between D_{01} and D_{02}) are expected to be mass dependent. In contrast the effect of the $C_{2v}\rightarrow C_s$ broken symmetry on the rovibronic density puts ^{17}O and ^{18}O [or (746) and (846)] on the same foot. Note that the same broken symmetry argument is used in the two existing models.[32,36] However, their respective quantitative analysis using *ad hoc* parameters is not convincing.

VI. CONCLUSION

Using high-resolution LIF spectrum we have determined the line densities of six isotopologues at energies $\sim 2-4\ cm^{-1}$ below the dissociation threshold. A statistical analysis of the corresponding rovibronic density, energy spacing, and rovibronic transition intensities has been made. The observed intensity distributions are in agreement with the Porter-Thomas distribution. This distribution allows one to estimate the number of missing levels, and therefore to determine and compare the rovibronic and the vibronic densities. The four symmetric NO_2 isotopologues, $^{16}O^{14}N^{16}O$, $^{18}O^{14}N^{18}O$, $^{16}O^{15}N^{16}O$, and $^{18}O^{15}N^{18}O$ have, respectively, a sum of $J=1/2$ and $J=3/2$ rovibronic densities of 18 ± 0.8, 18.3 ± 1.4, 18.4 ± 2.7, and $19.8\pm3.5/cm^{-1}$, while for the two asymmetric isotopologues, $^{18}O^{14}N^{16}O$ and $^{18}O^{15}N^{16}O$, the corresponding densities are 20.9 ± 4.5 and $23.6\pm5.6/cm^{-1}$. The corresponding vibronic densities are in agreement only if we include both the merging of symmetry species (from those of C_{2v} to those of C_s) and the contribution of the long-range tail(s) of the potential-energy surface along the dissociation coordinate. Does the observed difference between the symmetric and asymmetric NO_2 rovibronic densities imply

that there is a MIF effect occurring during NO_2 photolysis? Whereas there is considerable oxygen isotopic data for ozone formation (and destruction), there is no experimental or *in situ* data on the oxygen isotopic composition of NO_2. Recent isotope measurements of oxygen in tropospheric HNO_3, which is mainly derived from the three-body reaction NO_2+OH+M, have shown a very large oxygen isotopic effect, however the ^{17}O enrichment has been attributed to the transfer of oxygen atoms by ozone to NO during its oxidation to NO_2 even if a direct MIF from NO_2 cannot be ruled out. Photolysis experiments show that photolytic destruction of ozone in the visible follows normal mass dependency[50] and the body of theoretical work[34,40,51,52] assumes that the recombination ($O+O_2+M$) is the source of the anomalous isotope effect. This would suggest that NO_2 isotopologue photolysis would also follow mass-dependent behavior but that of the recombination reaction NO+O may be a MIF process. The recombination reaction is not important in the troposphere so that the suggested MIF transfer mechanism during NO oxidation is still valid. However, the NO+O recombination is an important sink of NO in the stratosphere where oxygen atom number densities are significant. Ionov *et al.*[48] suggested that the rovibronic density near D_0 was the result of a dynamical effect near the transition from the bound to unbound molecule and this concept has been refined using the dipole-dipole dipole-quadrapole model described by Heilliette *et al.*[53] However, as the photon energy increases additional exit channels of larger angular momentum open, the transition state tightens (because of the centrifugal contribution to the potential), and such subtle density anomalies are expected to vanish.[9,47] Future work is necessary to more clearly address the isotopic behavior of NO_2 during photolysis and recombination reactions.

[1] J. C. D. Brand, W. H. Chan, and J. L. Hardwick, J. Mol. Spectrosc. **56**, 309 (1975).
[2] A. Delon, R. Jost, and M. Jacon, J. Chem. Phys. **114**, 331 (2001).
[3] A. Delon and R. Jost, Chem. Phys. **110**, 4300 (1999).
[4] R. Georges, A. Delon, F. Bylicki, R. Jost, A. Campargue, A. Charvat, M. Chenevier, and F. Stoeckel, Chem. Phys. **190**, 207 (1995).
[5] R. Jost, M. G. Vergniory, and A. Campargue, J. Chem. Phys. **119**, 2590 (2003).
[6] J. Miyawaki, K. Yamanouchi, and S. Tsuchiya, J. Chem. Phys. **101**, 4505 (1994).
[7] A. Perrin, C. Camy-Peyret, J. M. Flaud, and P. Luc, J. Mol. Spectrosc. **88**, 237 (1981).
[8] B. Abel, B. Kirmse, J. Troe, and D. Schwarzer, J. Chem. Phys. **115**, 6522 (2001).
[9] A. Delon and R. Jost, J. Chem. Phys. **95**, 5686 (1991).
[10] A. Delon, R. Jost, and M. Lombardi, J. Chem. Phys. **95**, 5701 (1991).
[11] I. Bezel, D. Stolyarov, and C. Wittig, J. Phys. Chem. A **103**, 10268 (1999).
[12] S. A. Reid, A. Sanov, and H. Reisler, Faraday Discuss. **129**, ■ (1995).
[13] S. A. Reid and H. Reisler, Ann. Rev. Phys. Chem. **47**, 495 (1996).
[14] S. A. Reid and H. Reisler, J. Chem. Phys. **101**, 5683 (1994).
[15] P. I. Ionov, I. Bezel, S. I. Ionov, and C. Wittig, Chem. Phys. Lett. **272**, 257 (1997).
[16] C. F. Jackels and E. R. Davidson, J. Chem. Phys. **65**, 2941 (1976).
[17] R. Jost, M. Joyeux, and M. Jacon, Chem. Phys. **283**, 17 (2002).
[18] B. Kirmse, A. Delon, and R. Jost, J. Chem. Phys. **108**, 6638 (1998).
[19] R. Jost, Int. J. Quantum Chem. **64**, 571 (1997).
[20] A. Delon, R. Georges, and R. Jost, J. Chem. Phys. **103**, 7740 (1995).
[21] R. Jost, J. Nygard, A. Pasinski, and A. Delon, J. Chem. Phys. **105**, 1287 (1996).
[22] A. Delon, S. Heilliette, and R. Jost, Chem. Phys. **238**, 465 (1998).
[23] S. Heilliette, A. Delon, R. Jost, S. Y. Grebenschikov, R. Schinke, B. Abel, and J. C. Rayez, Z. phys. Chem. **215**, 1069 (2001).
[24] G. Michalski, Z. Scott, M. Kabiling, and M. Thiemens, Geophys. Res. Lett. **30**, 1870 (2003).
[25] M. H. Thiemens, J. Savarino, J. Farquhar, and H. Bao, Acc. Chem. Res. **34**, 645 (2001).
[26] C. C. W. Lee and M. H. Thiemens, J. Geophys. Res. **106**, 17359 (2001).
[27] M. H. Thiemens, Science **283**, 341 (1999).
[28] R. N. Clayton and T. K. Mayeda, Geochim. Cosmochim. Acta **63**, 2089 (1999).
[29] I. A. Franchi, L. Baker, J. C. Bridges, I. P. Wright, and C. T. Pillinger, Philos. Trans. R. Soc. London, Ser. A **359**, 2019 (2001).
[30] M. H. Thiemens and J. E. Heidenreich III, Science **219**, 1073 (1983).
[31] K. Mauersberger, D. Krankowsky, and C. Janssen, Space Sci. Rev. **106**, 265 (2003).
[32] K. Mauersberger, B. Erbacher, D. Krankowsky, J. Gunther, and R. Nickel, Science **283**, 370 (1999).
[33] Y. Q. Gao and R. A. Marcus, Science **293**, 259 (2001).
[34] B. C. Hathorn and R. A. Marcus, J. Chem. Phys. **111**, 4087 (1999).
[35] G. I. Gellene, Science **274**, 1344 (1996).
[36] J. J. Valentini, J. Chem. Phys. **86**, 6757 (1987).
[37] F. Robert and C. Camy-Peyret, Ann. Geophys. **19**, 229 (2001).
[38] S. M. Anderson, J. Morton, and K. Mauersberger, Chem. Phys. Lett. **156**, 175 (1989).
[39] S. Y. Grebenshchikov, R. Schinke, P. Fleurat-Lessard, and M. Joyeux, J. Chem. Phys. **119**, 6512 (2003).
[40] D. Babikov, B. K. Kendrick, R. B. Walker, R. T. Pack, P. Fleurat-Lesard, and R. Schinke, J. Chem. Phys. **119**, 2577 (2003).
[41] D. Babikov, B. K. Kendrick, R. B. Walker, R. Schinke, and R. T. Pack, Chem. Phys. Lett. **372**, 686 (2003).
[42] G. Michalski, R. Jost, D. Sugny, M. Joyeux, and M. Thiemens, J. Chem. Phys. **121**, 7153 (2004).
[43] H. D. Sharma, R. E. Jervis, and K. Y. Wong, J. Phys. Chem. **74**, 923 (1970).
[44] P. R. Bunker and Jensen, Per Molecular symmetry and spectroscopy NRC Research Press (1998).
[45] R. Georges, A. Delon, and R. Jost, J. Chem. Phys. **103**, 1732 (1995).
[46] T. A. Brody, J. Flores, J. B. French, P. A. Mello, A. Pandey, and S. S. M. Wong, Rev. Mod. Phys. **53**, 385 (1981).
[47] B. M. Toselli and J. R. Barker, J. Chem. Phys. **91**, 2239 (1989).
[48] S. I. Ionov, H. F. Davis, K. Mikhaylichenko, L. Valachovic, R. A. Beaudet, and C. Wittig, J. Chem. Phys. **101**, 4809 (1994).
[49] S. I. Ionov, G. A. Brucker, C. Jaques, Y. Chen, and C. Wittig, J. Chem. Phys. **99**, 3420 (1993).
[50] S. Chakraborty and S. K. Bhattacharya, J. Chem. Phys. **118**, 2164 (2003).
[51] Y. Q. Gao and R. A. Marcus, Science **293**, 259 (2001).
[52] R. Schinke and P. Fleurat-Lessard, J. Chem. Phys. **122**, ■ (2005).
[53] S. Heilliette, A. Delon, P. Dupre, and R. Jost, Phys. Chem. Chem. Phys. **3**, 2268 (2001).